

## ARTICLE

# Gelation properties of self-assembling *N*-acyl modified cytidine derivatives

Cite this: DOI: 10.1039/x0xx00000x

K. J. Skilling,<sup>a</sup> A. Ndungu,<sup>a</sup> B. Kellam,<sup>a</sup> M. Ashford,<sup>b</sup> T. D. Bradshaw,<sup>a</sup> and M. Marlow<sup>a</sup>

Received 00th January 2012,

Accepted 00th January 2012

DOI: 10.1039/x0xx00000x

[www.rsc.org/](http://www.rsc.org/)

In this study we report the synthesis of new cytidine derived gelators possessing acyl chains of different lengths. These low molecular weight gelators were shown to form self-supporting gels at 0.5 % (w/v) in binary systems of aqueous miscible polar organic solvent and water. The representative gels were studied using rheology and their fibrillar structure confirmed by TEM imaging and FTIR. We further demonstrated the use of these gels as potential drug delivery platforms by monitoring release characteristics of both high and low molecular weight fluorescently labelled tracers.

## Introduction

Progress in the field of low molecular weight gelators (LMWGs) is motivated by the numerous potential industrial and medical applications. Their attractive self-assembling properties and associated mechanical properties make them ideal for use in cosmetics, medicines and foods.

The self-assembled 3D fibrillar network of a LMWG is stabilised by non-covalent molecular interactions; hydrogen bonding,  $\pi$ - $\pi$  stacking, hydrophobic forces and electrostatic interactions. These interactions make LMWGs particularly advantageous for drug delivery as they will gelate under mild conditions such as subtle changes in pH or solvent polarity. Many examples of chemical entities which form low molecular weight gels by these processes exist<sup>1, 2</sup> of which di and tri peptide amphiphiles<sup>3-5</sup> are most common, however, reports of gelators that are both biocompatible and applicable in the field of drug delivery are rare.<sup>6</sup>

Nucleoside derived LMWGs have received little interest for the specific purpose of drug delivery, however, the abundance of nucleosides in nature makes them inherently biocompatible and thus an ideal foundation for a drug delivery platform. Additionally, nucleosides contain specific functional groups that make them particularly suited to becoming LMWGs; the nucleobase forming intermolecular interactions in a perpendicular direction whilst hydrogen bonding and  $\pi$ - $\pi$  stacking brought about from the heterocyclic ring holds together higher order structures.

Moreover, there is already a literature precedent for using nucleosides as the foundation for LMWGs, where previous studies have reported modified nucleosides that gelate in water.<sup>7</sup> For many years it has been known that guanosine makes a good

hydrogelator in a K<sup>+</sup> dependent system.<sup>8</sup> More recent findings suggest that a similar K<sup>+</sup> deoxy-guanosine system forms much better gels with improved thixotropic properties compared to the guanosine counterparts.<sup>9</sup> Other gelators arise *via* modification of the ribose sugar, a strategy employed by Yun,<sup>10</sup> Godeau<sup>11</sup> and Moreau<sup>12</sup> and Xu<sup>13, 14</sup> who recently reported enzyme labile gelating structures derived from existing known peptide gelators, functionalised at the 5'-position of the nucleoside guanosine and the nucleobase uridine. Another route less often taken is modification of the nucleobase at the 5-position, an example of which is that taken by Park<sup>15</sup> to derivatise ribo- and deoxyuridine.

The chemical modification of cytidine (**Figure 1a**) is less commonly reported; one of the earliest reports of cytidine derived gelators was of 5-triazoldeoxycytidines however the report was brief and didn't contain any information regarding gelation procedures.<sup>16</sup> More recently azide modified cytidine derivatives were synthesised<sup>17</sup> and were found to gel at minimal concentrations of 0.3 % (w/v) however there are no other reported cytidine derived gelators.

Herein we report a new series of modified cytidine LMWGs derived by functionalisation with an acyl chain at the 4-*N*-position of the cytosine ring; we explore how a co-solvent volume fraction of either DMSO or ethanol and water affects gel mechanical strength and nanostructure; and we demonstrate the capacity of these gels to act as reservoirs for drug like materials.

## Results and Discussion

The nucleoside, cytidine, **1** consists of a hydrophilic sugar moiety and a cytosine nucleobase that we hypothesised would

possess the hydrogen bonding donor and acceptor groups necessary to create the one dimensional order required to initiate gelation.<sup>1</sup> Introduction of hydrophobicity i.e. with an acyl chain would generate the solvophobic forces also required for gelation. By adapting previous literature<sup>18</sup> used to synthesise other nucleoside conjugates we were able to selectively acylate the *N*-position of the nucleobase using a series of fatty acids *via* a simple one-pot procedure (**Figure 1b**) generating compounds **2-5**. The formation of an activated triazine ester favours the addition on the *N*-position over the less nucleophilic 5'-position. Each of these compounds was synthesised with a yield of 39 – 60 % and with > 95 % purity *via* RP-HPLC.

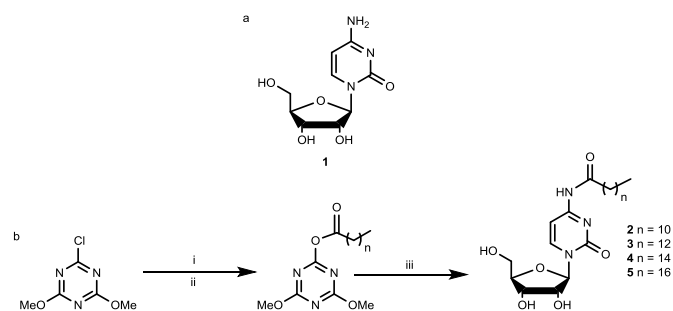


Figure 1: a) Structure of Cytidine and b) Reagents and conditions i. *n*-methylmorpholine,  $\text{CH}_2\text{Cl}_2$ , 0 °C, 1 h; ii. Fatty acid, 0 °C, 2 h, iii. Cytidine, DMF, 50°C, 12-24h.

None of the conjugates **2-5** were found to dissolve in water directly thus, gelation tests were conducted using a binary mixture of aqueous miscible organic solvent (dimethylsulfoxide (DMSO)<sup>19</sup> or ethanol) and water.

DMSO is currently the most common solvent used to solubilise gelators prior to gelation and is usually used sparingly, due to toxicity levels. However, for a cancer drug delivery platform increased concentrations of DMSO are potentially advantageous. DMSO has been shown to reduce growth of a human ovarian carcinoma (HOC-7) cell line reversibly in a dose- and time dependent manner<sup>20</sup> and to reduce the tumourigenicity of human pancreatic cell lines.<sup>21</sup> Conversely, few papers exist that claim to use ethanol as a gelating medium. A rare, recent example uses a gel formulated with 40 % (v/v) ethanol to demonstrate the enhanced release profile of indomethacin.<sup>22</sup> Additionally, ethanol has been used extensively as a pharmaceutical co-solvent for solubilisation of poorly soluble drugs,<sup>23</sup> and has associated clinical guidance recommending intra-tumoural ethanol injection in oesophageal, gastric and pancreatic tumours as a method of ablation.<sup>24</sup> Hence, we believe ethanol would enhance the therapeutic effect of a localised, targeted drug delivery system.

LMWGs are commonly formed by using a low percentage (0.1 – 5 % (w/v)) of gelator molecule in an appropriate medium. In recent times an increased understanding in the way LMWGs should be designed means molecular properties can be tailored

so that gels can be consistently formed at concentrations towards the lower limit of the accepted range. Many examples of gelators that assemble in a low concentration range (0.02 – 0.5 % (w/v)) exist.<sup>1</sup> Here, we report the gelation of conjugates **2-5** in different solvent volume fractions ( $\Phi_{\text{SOL}}$ ) (0.05 to 0.50) and with a low final compound concentration of 0.5 % (w/v). The qualitative stability of the gels was analysed by ‘stable to inversion’ assessment of the container, resulting from gels prepared *via* a heating-cooling method; when the liquid no longer flowed it was concluded that gelation had occurred. (**Figure S2, ESI**)

As reported elsewhere for dipeptides,<sup>25, 26</sup> the addition of water to the gelator containing organic phase results in the appearance of a turbid solution that gradually, over time clarifies to give a stable gelator. This too was noticed for our *N*-acyl nucleoside series **2-5** (**Table 1**). It is hypothesised that this may be due to restructuring of an initial self-assembled structure from many irregular aggregates into more highly ordered structures.<sup>25</sup> It was noticed that the more lipophilic character the nucleoside conjugate possessed the less stable the gels were to inversion. This was particularly apparent in gels of **4** and **5** where across both DMSO and ethanol series ‘only one visually stable gelator was seen at  $\Phi_{\text{EtOH}}$  0.40 and  $\Phi_{\text{DMSO}}$  0.50, respectively.

No gelation was seen at low solvent volume fractions of 0.05 in any conjugates though the presence of weak gels became apparent at  $\Phi_{\text{SOL}}$  0.10 in gels of **2** and **3**. However, an increased turbidity was seen in these samples, this was particularly apparent in those gels containing **2**, where clarification didn’t seem to happen even at  $\Phi_{\text{SOL}}$  0.50. In gels of **3** a visually stable clarified sample occurred at  $\Phi_{\text{SOL}}$  0.40. Additional stability to inversion was noted for samples of **3** prepared in ethanol over their DMSO counterparts. This observation may be attributed to the disruption in hydrogen bonding caused by DMSO. We have shown here that by creating a binary mixture of solvent (DMSO or ethanol) and water, we could reproducibly promote gelation and have demonstrated an increased propensity for gelation of conjugate **3** in organic solvent/water when compared to series **2, 4** and **5**.

| $\Phi_{\text{SOL}}$ | Conjugate |    |    |    |         |    |    |    |
|---------------------|-----------|----|----|----|---------|----|----|----|
|                     | DMSO      |    |    |    | ethanol |    |    |    |
|                     | 2         | 3  | 4  | 5  | 2       | 3  | 4  | 5  |
| 0.05                | P         | P  | P  | P  | P       | P  | P  | P  |
| 0.10                | WG        | P  | P  | P  | WG      | WG | P  | P  |
| 0.20                | WG        | WG | WG | WG | WG      | WG | WG | WG |
| 0.30                | WG        | WG | WG | WG | G       | G  | WG | WG |
| 0.40                | WG        | G  | WG | WG | WG      | G  | G  | WG |
| 0.50                | G         | G  | WG | G  | WG      | G  | WG | WG |

Table 1: Representative data table for Gels of 2-5 in DMSO and ethanol with solvent volume fractions ( $\Phi_{\text{SOL}}$ ) from 0.05 to 0.50 and with final compound concentrations of 0.5 % (w/v) where G: Gel; WG: Weak Gel P: Precipitate

To further understand the stability of the gel to inversion, samples made with 0.5 % (w/v) conjugate **3** (cytidine-*N*-myristoyl) were analysed by oscillatory rheology to quantify the mechanical strength of each gel and to identify the optimum solvent ratio. The viscoelastic properties of the gels were found

to depend upon the  $\Phi_{\text{SOL}}$  in the system (Figure 2) a feature that has been reported previously for dipeptide hydrogels, of concentrations up to  $\Phi_{\text{DMSO}}$  0.40.<sup>25</sup> Here we found a very good correlation between visual stability and the associated quantitative mechanical strengths. We noted that above  $\Phi_{\text{SOL}}$  0.50 the sample behaves more like a liquid owing to the solubility of the compound in organic solvent. The storage modulus ( $G'$ ) of the gels generally increased with increasing solvent fraction up to  $\Phi_{\text{SOL}}$  0.40 giving a maximum of 3500 Pa. The mechanical properties ( $G'$  and  $G''$ ) of the gels were reproducible (means and standard deviations are of 3 independent samples). In every case the  $G'$  exceeded  $G''$  by at least an order of magnitude; a feature significant amongst low molecular weight gelators.<sup>27</sup> Values of  $G'$  and  $G''$  of  $\Phi_{\text{EtOH}}$  0.40 were found not to be dependent on oscillatory frequency between 1 and 100 rad/s, an indicator of a strong cross-linked fibrillar structure. However, a frequency dependency was seen for the corresponding  $\Phi_{\text{DMSO}}$  0.40 sample indicating a weaker intermolecular network.

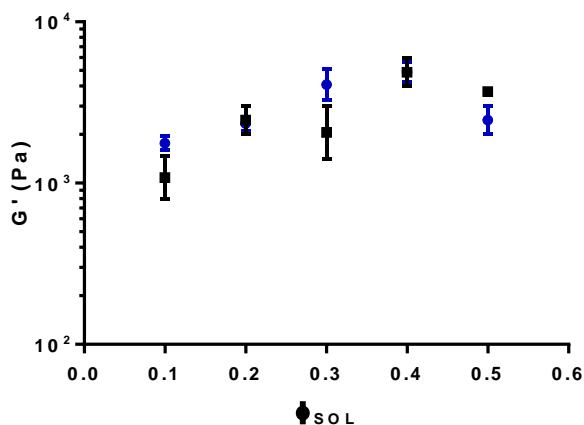


Figure 2:  $G'$  values of **3** (0.5 % (w/v)) in DMSO (black square) and ethanol (blue circle) at 1 % strain i.e. in the linear viscoelastic region. All measurements were carried out in triplicate and the mean calculated. Error bars represent standard deviation.

To investigate further the above oscillatory rheology data, we probed the molecular interactions by FTIR. (Figure 3c) IR peaks at 1681 and 1642  $\text{cm}^{-1}$  represent the amide I region of **3**.<sup>28</sup> As the volume fraction of solvent was increased from  $\Phi_{\text{EtOH}}$  0.20 to 0.30 a clear change in the molecular packing was observed. The peak at 1681 was seen to broaden and attenuate, shifting slightly from 1681  $\text{cm}^{-1}$  to 1678  $\text{cm}^{-1}$ . An additional shift was seen from the peak at 1652  $\text{cm}^{-1}$  shifting and broadening into a peak at 1642  $\text{cm}^{-1}$ . The peak shifts and broadening observed *via* FTIR are indicative of hydrogen bonding and have been observed for other gelating molecules.<sup>15, 29</sup> These findings imply the change from 'free' single molecules to a hydrogen bonded network.

This hydrogen bonded network is characteristic of a cross-linked LMWG, a feature that was further supported by scanning electron microscopy (SEM) and transmission electron microscopy (TEM). (Figure 3a, b) At a fraction  $\Phi_{\text{EtOH}}$  0.40 we saw cross-linked fibrillar structures, again a structural feature of a LMW gelating network. The fibre diameters were in the region of 15-25 nm with a length of up to 100's microns. Further observations of the TEM imaging suggested that the fibrillar networks contained a number of microscopic cavities, which could potentially be used for encapsulation and controlled drug release. However due to sample preparation and the high vacuum drying conditions involved we can't assume

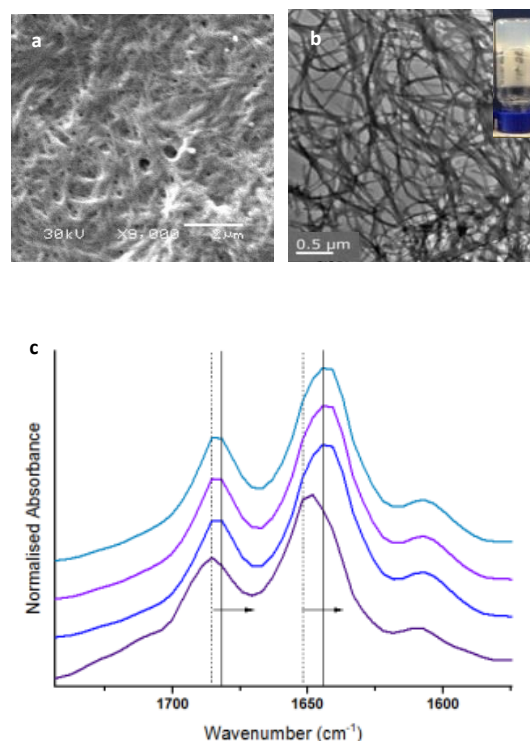


Figure 3: a) SEM and b) TEM image of **3** ( $\Phi_{\text{EtOH}}$  0.40) with a sample vial inversion and c) FTIR top to bottom  $\Phi_{\text{EtOH}}$  0.50, 0.40, 0.30 and 0.20. Spectra are off set to demonstrate peak shifts and peak broadening.

that these features are completely representative of the matrix in its hydrated state. To examine the above observation we examined the gel matrix using a series of *in-vitro* release studies. The gels of **3** ( $\Phi_{\text{EtOH}}$  0.40) were self-assembled in the presence of large and small molecular weight fluorescent molecules. The lowest molecular weight fluorescent molecule was fluorescein, possessing a molecular mass of 332 Da, the second, a higher molecular mass fluorescent, fluorescein isothiocyanate (FITC)-Dextran with a molecular mass of 4 kDa and the final FITC Dextran 10 (10 kDa). A quantity (5 mL) of buffer was introduced to the top of the gel and aliquots (150  $\mu\text{L}$ ) removed from the buffer at intervals (1, 8 and 24 h) and we

were then able to measure the fluorescence and calculate the percentage of molecules released. (**Figure 4**)

Our studies demonstrated that 88 % of fluorescein molecules are released within 24 h from the gel matrix, FITC Dextran 4 showed a moderate 66 % release whilst the larger FITC-Dextran 10 molecules demonstrated very little release during the same time frame. This could be attributed to the close packing of the fibres within the gel matrix significantly retarding the free diffusion of these larger molecules. We can therefore assume that the gel will retain molecules with a large mass and molecules with smaller masses (100's Da) will be released in agreement with others who have also shown similar retention of higher molecular mass molecules from a gelating dipeptide based hydrogel.<sup>4,30</sup> Such properties suggest potential applications in drug delivery for example as a depot for intratumoural drug release.

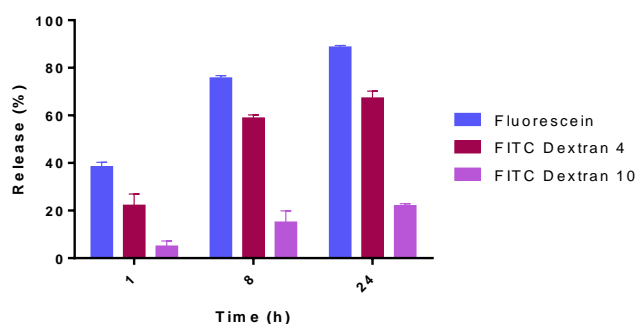


Figure 4: Percentage release of Fluorescein (0.15 mM), FITC Dextran 4 (0.06 mM) and FITC Dextran 10 (0.01 mM) through the gel matrix. This figure is representative of 5 repeat release experiments, n = 4 in each experiment.

To demonstrate the biocompatibility and applicability of these cytidine-*N*-myristoyl conjugates as the foundation of an intratumoural drug delivery platform, the *in-vitro* toxicity was examined *via* mammalian cell growth inhibition assays and the concentration inhibiting growth by 50 % (GI<sub>50</sub>) determined. The conjugate **3** was incubated with human breast (MCF-7) and colorectal (HCT-116) carcinoma cells for 72 h at 37 °C. The results (**Figure 5**) suggest a comparable toxicity between our conjugates and the parent compound cytidine in both cell lines with the conjugate demonstrating GI<sub>50</sub> values of 6.37 mM and 7.78 mM respectively.

## Experimental Section

### Materials

All chemicals and solvents were purchased from commercial suppliers and used without further purification. Synthetic reactions were performed in oven-dried glassware and magnetically stirred. Thin layer chromatography (TLC) was

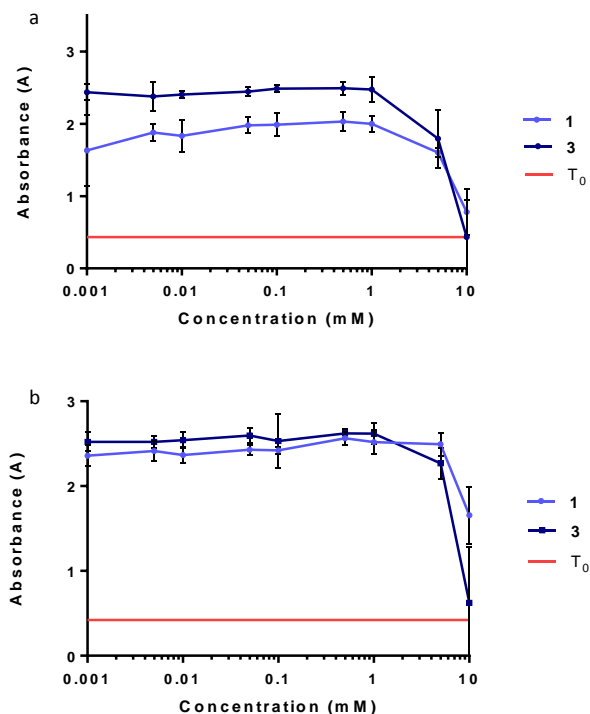


Figure 5: Growth Inhibition data on a) MCF-7 cells and b) HCT-116. T<sub>0</sub> represents 100% growth inhibition.

performed on Merck Kieselgel 60 F254 plates. All compounds were visualized either by UV light source (254 nm) or by staining in potassium permanganate solution. Silica column chromatography was carried out using silica gel, Merck Kieselgel 60, 230-400 mesh (Merck KGaA, Darmstadt, Germany).

### Methods

**General Methods** <sup>1</sup>H NMR spectra were recorded on a Bruker 400 Ultrashield at 400 MHz at 25 °C. <sup>13</sup>C NMR spectra were recorded on a Bruker 400 Ultrashield at 100 MHz at 25 °C. Solvent used for NMR analysis was DMSO-*d*<sub>6</sub> ((CHD<sub>2</sub>)<sub>2</sub>SO at δH 2.50 ppm, (CD<sub>3</sub>)<sub>2</sub>SO at 39.52 ppm). Chemical shifts (δ) are recorded in parts per million (ppm). Coupling constants (J) are recorded in Hz (rounded to one decimal place) and any significant multiplicities described by singlet (s), doublet (d), triplet (t), quadruplet (q) and multiplet (m). Spectra were assigned using COSY and HSQC sequences. High resolution mass spectra (HRMS) – time of flight electrospray (TOF ES +/-) were recorded on a Waters 2795 separation module micromass LCT platform. Infrared spectra were obtained using Nicolet Fourier-transformed infra-red (FTIR) spectrophotometer. Reverse phase high performance liquid chromatography (RP-HPLC) was performed using a Waters 2767 sample manager, Waters 2525 binary gradient module and visualised at 254 nm with a Waters 2487 dual wavelength absorbance detector. Spectra were analysed using MassLynx.

Analytical RP-HPLC was performed using a YMC-Pack C8 column (150 mm x 4.6 mm x 5  $\mu$ m) at a flow rate of 1 mL/min. The retention time ( $t_R$ ) of the final product is reported using an analytical method of 0 – 1 min 5 % solvent B in solvent A, 2 – 26 min gradient of 5 % to 90 % solvent B in solvent A, 27 – 35 min held at 90 % solvent B in solvent A, 35 - 36 min 90 % to 5 % solvent B in solvent A, 36 - 38 min held at 5 % solvent B in solvent A (solvent A = 0.05 % TFA in H<sub>2</sub>O, solvent B = 0.05 % TFA in 9:1 v:v CH<sub>3</sub>CN:H<sub>2</sub>O).

**Synthesis of *N*-acyl cytidine derivative, 3** To a solution of 2-chloro-4,6-dimethoxy-1,3,5-triazine (CDMT, 20 mmol, 3.50 g) in anhydrous CH<sub>2</sub>Cl<sub>2</sub> (60 mL) at 0 °C, *N*-methylmorpholine (NMM, 27.2 mmol, 2.75 g) was added with continuous stirring until a white suspension had formed. The mixture was then left to stir for 1 h. Myristic acid (20 mmol) was added directly into the mixture as a solution in anhydrous DMF (20 mL) and stirred for a further hour. A solution of cytidine (20 mmol, 4.86 g) in anhydrous DMF (20 mL) was made up at 0 °C. The cold triazine solution was added drop wise to the cooled cytidine solution over 30 mins, before heating to 50 °C and stirring for 14 - 24 h. The cooled solution was evaporated *in vacuo* before adding water and triturating to remove excess CDMT, NMM and cytidine. This was followed by trituration with CH<sub>2</sub>Cl<sub>2</sub> to remove any excess myristic acid. The products were purified using flash silica column chromatography, eluting at 5 - 7 % methanol in CH<sub>2</sub>Cl<sub>2</sub>.

**3** <sup>1</sup>H NMR (DMSO-*d*<sub>6</sub>, 400 MHz)  $\delta$  0.85 (t,  $J$  = 7.2 Hz, 3H, CH<sub>3</sub>), 1.24 (s, 20H, CH<sub>2</sub>-(CH<sub>2</sub>)<sub>10</sub>-CH<sub>3</sub>), 1.53 (m, 2H, C=O-CH<sub>2</sub>-CH<sub>2</sub>), 2.38 (t,  $J$  = 7.3 Hz, 2H, C=O-CH<sub>2</sub>), 3.56 - 3.61 (m, 1H, CH<sub>2</sub>-OH), 3.71 - 3.76 (m, 1H, CH<sub>2</sub>-OH), 3.89 - 3.90 (m, 1H, CH-CH<sub>2</sub>-OH), 3.93 - 3.98 (m, 2H, 2(CH-OH)), 5.03 (d,  $J$  = 5.7 Hz, 1H, N-CH-CH-CH-OH), 5.14 (t,  $J$  = 5.1 Hz, 1H, CH<sub>2</sub>-OH), 5.46 (d,  $J$  = 5.1 Hz, 1H, N-CH-CH-OH), 7.20 (d,  $J$  = 7.5 Hz, 1H, N-CH-CH-C), 8.40 (d,  $J$  = 7.6 Hz, 1H, N-CH-CH-C), 10.83 (s, 1H, NH). <sup>13</sup>C NMR (DMSO-*d*<sub>6</sub>, 100 MHz)  $\delta$  13.92, 22.06, 24.4, 28.42, 28.67, 28.83, 28.98, 29.02, 31.26, 36.33, 59.91, 68.65, 74.51, 84.18, 90.13, 95.20, 145.31, 154.66, 162.30, 173.92. HRMS calculated for C<sub>23</sub>H<sub>40</sub>N<sub>3</sub>O<sub>6</sub><sup>+</sup> 454.2192 (M+H)<sup>+</sup>; found 454.2928. Analytical RP-HPLC  $t_R$  = 23.9 min, Yield: 46.0 %, 99.7 % purity.

**Preparation of Gels** In all cases, gels of each amphiphilic conjugate were prepared as follows; **2 - 5** were weighed using an A and D GR-202 semi micro-analytical balance into 1.5 ml sample vials. Solvent (DMSO or ethanol, 1 mL) was added to create stock solutions at 10 % (w/v) This solution was then sonicated in a Sonicor Ultra-sonic bath for 1 - 2 minutes before heating to 60 °C to dissolve the compound fully. A small aliquot (25  $\mu$ L) of this stock solution was transferred to another 1.5 mL heated vial before adding additional solvent and finally pre heated (60 °C) ultra-purified water. The sample was then left to cool down to room temperature in the heating plate and left standing for 18 h.

**Fourier Transformed Infrared Spectroscopy (FTIR)** IR spectra were collected using an Agilent Cary 630 spectrometer with ATR crystal at 8 cm<sup>-1</sup> resolution, averaging over 32 scans from 4000 cm<sup>-1</sup> to 650 cm<sup>-1</sup>. The gels of **3** (0.5 % (w/v)) used for IR measurements were prepared in a mixture of EtOD-*d*<sub>6</sub> and D<sub>2</sub>O as described above. After being allowed to gel overnight, samples were placed onto an ATR crystal and scanned.

**Rheology** Rheology experiments were carried out using an Anton Paar MCR302 Modular Compact Rheometer. A four-bladed vane geometry was used with a diameter of 8.5 mm and length 8.5 mm in a cup with a diameter of 14.5 mm. For the strain and frequency measurements the solution of gelator was prepared in a 7 mL sterilin plastic sample vial and gelation promoted in the same manner as in the standard gelation procedure described above (to make a volume of 2 mL). Once the gel had been prepared, the sample vial was mounted in the lower plate (cup) of the rheometer, the vane (attached to the upper part) was lowered into place. This arrangement gave a sample depth of approximately 16 mm in the 14.5 mm diameter cup which allowed positioning of the vane in the centre of the sample.<sup>31</sup> All strain amplitude measurements were made within the linear viscoelastic region of the gel sample where the storage modulus and loss modulus ( $G'$  and  $G''$  respectively) are independent of the strain amplitude. The  $G'$  and  $G''$  were measured at a frequency of 10 rad s<sup>-1</sup>. Frequency scans were executed from 1 rad s<sup>-1</sup> to 100 rad s<sup>-1</sup> under a strain of 1 %.

**Transmission Electron Microscopy (TEM Imaging)** The morphology of the self-assembled fibres was assessed using a JEOL JEM 2100 transmission electron microscope (TEM). To prepare samples, a small amount of gel was dispersed in 200  $\mu$ L of ultra-purified water and pipetted on to a carbon-coated copper grid (No. 400). Excess sample was blotted with Whatman 50 filter paper. The grid was subjected to high vacuum prior to inserting into the machine and imaging at an accelerated voltage of 200 kV.

**Growth Inhibition Studies** Cells were seeded at a density of 3 x 10<sup>3</sup> per well into 96-well microtiter plates and allowed to adhere for 24 h before test agent was introduced (0.1 nM – 100  $\mu$ M,  $n$  = 8). Serial dilutions were prepared in RPMI medium prior to each assay. At the time of agent addition and following 72 h exposure, 3-(4,5-dimethylthiazol-2-yl)-2,5-diphenyltetrazolium bromide (MTT) was added to each well (final concentration 400  $\mu$ g/mL). Incubation at 37 °C for 3 h allowed reduction of MTT by viable cells (mitochondrial dehydrogenases) to insoluble formazan crystals. Well supernatants were removed, and intracellular formazan solubilized by addition of DMSO (150  $\mu$ L). Absorbance was read at 550 nm using a Perkin Elmer plate reader. Non-linear regression analysis was used to calculate compound concentrations required to inhibit 50 % of cell growth (GI<sub>50</sub>).

**In-vitro release kinetics** Gels ( $\Phi_{\text{EtOH}}$  0.40) containing fluorescent dyes were prepared in 7 mL sterilin cups up to the volume of 2 mL with the dye phase replacing the aqueous phase in each instance. Stock solutions of each dye were prepared so that the fluorescent output would be within the linear region of the calibration curves (0.15 mM Fluorescein and 0.06 mM Fluorescein isothiocyanate (FITC) Dextran 4 kDa and 0.1 mM FITC Dextran 10 kDa). Having prepared the gels using the standard method, the gel volume was allowed to stand for 18 h to allow time for complete gelation. Ultra-purified water (5 mL) was gently placed on top of each gel and the initial time point taken (150  $\mu\text{L}$ ,  $T_0$ ), subsequent readings (150  $\mu\text{L}$ ) were taken at further time points and the fluorescence measured (excitation of 485 nm with the emission measured at 521 nm) using a Perkin Elmer plate reader

## Conclusions

We have designed a novel series of low molecular weight nucleoside gelators derived *via* simple chemical modification of the *N*-position on the cytosine nucleobase and have shown how, when prompted by a change in solvent polarity, we observe a rapid gelation process resulting in the formation of a stable self-assembled cross-linked fibrillar network.

Through rheological testing, TEM imaging and FTIR we have demonstrated the importance of the solvent: water ratio to the self-assembly process. Specifically we have shown that a gel containing  $\Phi_{\text{EtOH}}$  0.40 displays enhanced self-assembly capabilities, arranging itself into an ordered highly cross-linked fibrillar structure with an increased mechanical strength. FTIR spectroscopy alluded to the critical importance of the amide functionality in the self-assembly process. Additionally, the possible application of such gels as reservoirs for both large and small bio macromolecular therapeutics was fully demonstrated. Furthermore, we proposed how this increased solvent ratio could be advantageous particularly for delivery of cancer therapeutics but may also hold additional applications for example in the field of dermatology. We therefore propose these cytidine gelators as useful chemical building blocks for new gelators in drug delivery.

## Acknowledgements

Support from Christine Grainger-Boulton for SEM imaging, Mike Fay at the Nottingham Nanotechnology and Nanoscience Centre (NNNC) for the TEM Imaging and Timothy Eason for consultation on FTIR is gratefully acknowledged. We are grateful to EPSRC (EP/I01375X/1) and AstraZeneca for funding.

## Notes and references

<sup>a</sup> School of Pharmacy, University of Nottingham, University Park, Nottingham, NG7 2RD, UK.

<sup>b</sup> AstraZeneca, Alderley Park, Macclesfield, Cheshire, SK10 4TG, UK

† Electronic supplementary information (ESI) available. Full  $^1\text{H}$  NMR,  $^{13}\text{C}$  NMR COSY, RP-HPLC and vial inversion available for all synthesised compounds.

1. K. J. Skilling, F. Citossi, T. D. Bradshaw, M. Ashford, B. Kellam and M. Marlow, *Soft Matter*, 2014, **10**, 237.
2. R. Weiss and P. Terech, *Molecular Gels: Materials with Self-assembled fibrillar networks*, Springer, 2006.
3. D. J. Adams, *Macromolecular Bioscience*, 2011, **11**, 160-173.
4. A. Mahler, M. Reches, M. Rechter, S. Cohen and E. Gazit, *Advanced Materials*, 2006, **18**, 1365-1370.
5. Y. M. Abul-Haija and R. V. Ulijn, in *Hydrogels in Cell-Based Therapies*, The Royal Society of Chemistry, 2014, pp. 112-134.
6. V. Allain, C. Bourgaux and P. Couvreur, *Nucleic Acids Res*, 2012, **40**, 1891-1903.
7. K. Araki and I. Yoshikawa, in *Low Molecular Mass Gelator*, Springer Berlin Heidelberg, 2005, vol. 256, ch. 107173, pp. 133-165.
8. W. Guschlbauer, D. Chantot Jf Fau - Thiele and D. Thiele, *J Biomol Struct Dyn*, 1990, **8**, 491-511.
9. B. Adhikari, A. Shah and H.-B. Kraatz, *Journal of Materials Chemistry B*, 2014.
10. Y. J. Yun, B. H. Park Sm Fau - Kim and B. H. Kim, *Chem Commun (Camb)*, 2003, 254-255.
11. G. Godeau and P. Barthelemy, *Langmuir*, 2009, **25**, 8447-8450.
12. L. Moreau, P. Barthélémy, M. El Maataoui and M. W. Grinstaff, *J Am Chem Soc*, 2004, **126**, 7533-7539.
13. D. Wu, J. Zhou, J. Shi, X. Du and B. Xu, *Chem Commun (Camb)*, 2014, **50**, 1992-1994.
14. D. Yuan, R. Zhou, J. Shi, X. Du, X. Li and B. Xu, *RSC Advances*, 2014, **4**, 26487-26490.
15. S. M. Park, B. H. Shen Y Fau - Kim and B. H. Kim, *Org Biomol Chem*, 2007, **5**, 610-612.
16. N. K. Andersen, L. Spáčilová, M. D. Jensen, P. Kočalka, F. Jensen and P. Nielsen, *Nucleic Acids Symposium Series*, 2008, **52**, 149-150.
17. D. J. Dodd, ND. Hudson, RHE., *Artificial DNA: PNA + XNA*, 2010, **1**, 90-95.
18. A. B. Rode, S. J. Son and I. S. Hong, *Bulletin of the Korean Chemical Society*, 2010, **31**, 2061-2064.
19. J. Raeburn, G. Pont, L. Chen, Y. Cesbron, R. Levy and D. J. Adams, *Soft Matter*, 2012, **8**, 1168-1174.
20. T. W. Grunt, C. Somay, M. Pavelka, A. Ellinger, E. Dittrich and C. Dittrich, *Journal of Cell Science*, 1991, 657-666.
21. L. J. McIntyre and Y. S. Kim, *European Journal of Cancer Clinical Oncology*, 1984, **20**, 265-271.
22. M. Rodrigues, A. C. Calpena, D. B. Amabilino, M. L. Garduno-Ramirez and L. Perez-Garcia, *Journal of Materials Chemistry B*, 2014, **2**, 5419-5429.
23. T. R. Joseph, in *Encyclopedia of Pharmaceutical Technology, Third Edition*, Taylor & Francis, 2013, vol. null, pp. 806-819.
24. W. G. Allum, S; Watson, A; Colin-Jones, D, *Gut.*, 2002, **1-23**.
25. R. Orbach, I. Mironi-Harpaz, L. Adler-Abramovich, E. Mossou, E. P. Mitchell, V. T. Forsyth, E. Gazit and D. Seliktar, *Langmuir*, 2012, **28**, 2015-2022.

26. A. M. Smith, R. J. Williams, C. Tang, P. Coppo, R. F. Collins, M. L. Turner, A. Saiani and R. V. Ulijn, *Advanced Materials*, 2008, **20**, 37-41.
27. P. Terech and R. G. Weiss, *Chemical Reviews*, 1997, **97**, 3133-3159.
28. A. Aggeli, M. Bell, N. Boden, J. Keen, P. Knowles, T. McLeish, M. Pitkeahly and S. Radford, *Nature*, 1997, 259-262.
29. L. Chen, J. Raeburn, S. Sutton, D. G. Spiller, J. Williams, J. S. Sharp, P. C. Griffiths, R. K. Heenan, S. M. King, A. Paul, S. Furzeland, D. Atkins and D. J. Adams, *Soft Matter*, 2011, **7**, 9721-9727.
30. S. Sutton, N. L. Campbell, A. I. Cooper, M. Kirkland, W. J. Frith and D. J. Adams, *Langmuir*, 2009, **25**, 10285-10291.
31. J. R. Stokes and J. H. Telford, *Journal of Non-Newtonian Fluid Mechanics*, 2004, **124**, 137-146.